

A Bayesian Hierarchical Model for Prediction of Latent Health States from Multiple Data Sources with Application to Active Surveillance of Prostate Cancer

R. Yates Coley^{a*}, Aaron J. Fisher^a, Mufaddal Mamawala^b

H. Ballentine Carter^b, Kenneth J. Pienta^{b,c,d}, and Scott L. Zeger^a

^aDepartment of Biostatistics, Johns Hopkins Bloomberg School of Public Health

^bJames Buchanan Brady Urological Institute, Johns Hopkins Medical Institutions

^cDepartment of Oncology, Johns Hopkins Medical Institutions

^dDepartment of Pharmacology and Molecular Sciences, Johns Hopkins Medical Institutions

June 26, 2022

*RYC is a postdoctoral research fellow in the Department of Biostatistics, John Hopkins Bloomberg School of Public Health (JHBSPH), Baltimore, MD 21205 (Email: ryc@jhu.edu). AJF is a PhD Candidate in the Department of Biostatistics, JHBSPH (fisher@jhu.edu). MM is a biostatistician at the James Buchanan Brady Urological Institute (JBBUI), Johns Hopkins Medical Institutions (JHMI), Baltimore, MD 21287 (mmamawa1@jhmi.edu). HBC is Director of Adult Urology and Professor, JBBUI, JHMI (hcarte1@jhmi.edu). KJP is Professor, JBBUI, Department of Oncology, and Department of Pharmacol-

Abstract

In this article, we present a Bayesian hierarchical model for predicting a latent health state from longitudinal clinical measurements. Model development is motivated by the need to integrate multiple sources of data to improve clinical decisions about whether to remove or irradiate a patient’s prostate cancer. Existing modeling approaches are extended to accommodate measurement error in cancer state determinations based on biopsied tissue and to allow observations to possibly be missing not at random. The proposed model enables estimation of whether an individual’s underlying prostate cancer is aggressive, requiring surgery and/or radiation, or indolent, permitting continued surveillance. These individualized predictions can then be communicated to clinicians and patients to inform decision making. We demonstrate the model with data from a cohort of low risk prostate cancer patients at Johns Hopkins University and assess predictive accuracy among a subset for whom we observe the true cancer state. Simulated data and R code is available at <https://github.com/rycoley/prediction-prostate-surveillance>.

Keywords: Latent class analysis; Missing data; Precision medicine; Prostate cancer prognosis; Risk classification

ogy and Molecular Sciences, JHMI (kpienta1@jhmi.edu). SLZ is Professor, Department of Biostatistics, JHBSPH (sz@jhu.edu). This research was supported by the Patrick C. Walsh Prostate Cancer Research Fund and a Patient-Centered Outcomes Research Institute (PCORI) Award (ME-1408-20318). The statements presented in this article are solely the responsibility of the authors and do not necessarily represent the views of the Patient-Centered Outcomes Research Institute (PCORI), its Board of Governors or Methodology Committee. The authors gratefully acknowledge Ruth Etzioni, Tom Louis, and Gary Rosner for their helpful comments.

1 Introduction

Medicine is in a period of transition. An ever-increasing amount of information is available on patients ranging from genetic and epigenetic profiles enabled by next-generation sequencing to moment-to-moment data collected by physical activity monitors. With this wealth of information comes the opportunity to provide more targeted healthcare including, for example, prediction of pre-clinical atherosclerosis [30], individualized cancer screening [36], sub-typing of scleroderma [39], and personalized cancer treatment [20]. In order to fully realize the promise of patient-focused medicine, principled statistical methods are needed that integrate data from a variety of sources in order to provide physicians and patients with relevant syntheses to inform their decision-making. These methods must also accommodate limitations common to data generated in an observational setting including measurement error and informative missing data patterns.

An excellent example of this challenge is low-risk prostate cancer diagnosis. Tumor lethality is an aspect of an individual's health state that is not directly observable but is manifest in multiple types of measurements including biomarkers, histology of biopsied tissue, genetic markers, and family history of the disease. Individualized predictions of the latent disease state are critical to guide treatment decisions. If the tumor is potentially lethal, immediate treatment, including surgery or radiation, can be life-saving. Yet, some tumors are indolent and not life-threatening. In this case, treatment is not recommended due to the risk of lasting side effects including urinary incontinence and erectile dysfunction [6].

Active surveillance (AS) offers an alternative to early treatment for individuals with lower risk disease [4, 25, 26, 41, 44, 46, 47]. Though AS regimes vary, the approach generally entails regular biopsies (e.g., annually) with intervention recommended upon detection of

higher risk histological features, as determined by the Gleason grading system [16, 17]. Biopsies with a Gleason score of 6 (the minimum for prostate cancer) indicate low risk disease while a Gleason score of 7 or above is considered “grade reclassification” to a higher risk [44]. Prostate-specific antigen (PSA), a blood serum biomarker of inflammation, is also routinely measured and may be used as the basis for a biopsy recommendation.

The success of AS programs depends on clinicians’ ability to identify tumors with metastatic potential with sufficient time for curative intervention to be effective. Biopsies used to characterize tumors typically sample less than one percent of the prostate tissue and so have imperfect sensitivity and specificity [10]. Existing decision support tools that predict biopsy outcomes for AS patients (including, most recently, Ankerst et al. (2015)) provide patients and physicians with valuable information to guide decisions about biopsy timing and frequency but are insufficient to directly address patients’ primary concerns about their tumors’ lethality. Patients and clinicians need predictions of the pathological make-up of the entire prostate to guide their decision-making.

With this application in mind, we have developed a Bayesian hierarchical model that enables prediction of an individual’s underlying disease state via joint modeling of repeated PSA measurements and biopsies. Specifically, we predict a binary cancer state– *indolent* or *aggressive*– with the latter defined as a true Gleason score of 7 or higher. Predictions are informed by a subset of patients for whom the true state is observed– patients who, either before or after grade reclassification, underwent elective prostatectomy and have post-surgery, entire-prostate Gleason score determinations. In this sense, cancer state operates as a partially-latent class in the proposed model [48].

An individual’s cancer state is assumed to be manifest in both the level and trajectory of PSA measurements as well as in the outcomes from repeated biopsies. These relationships are illustrated by the directed acyclic graph (DAG) in Figure 1(a). In the model we are

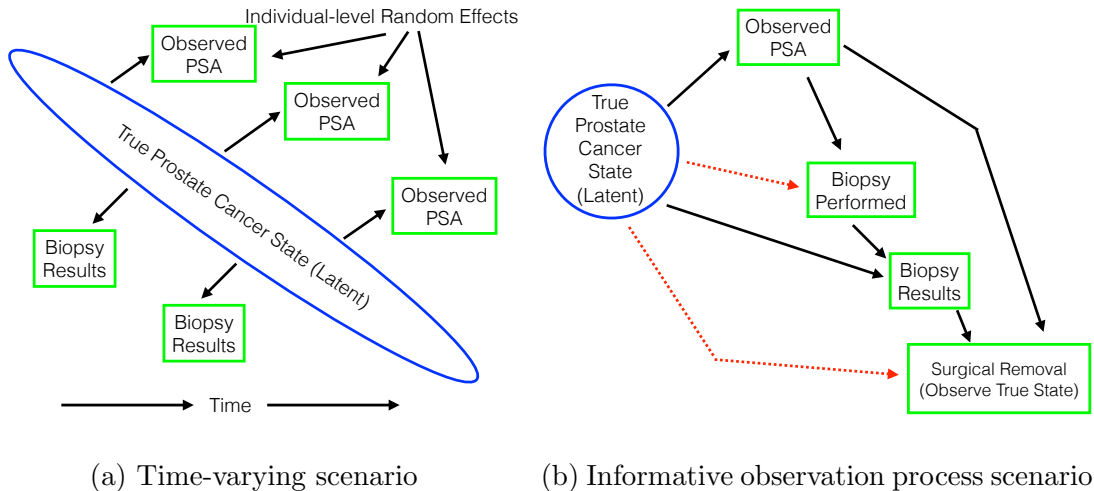


Figure 1: DAGs describing the relationships between latent class (circled) and observed outcomes (squared).

proposing, PSA measurements follow a multilevel model with mean effects of age varying across latent classes [15]. Then, time until reclassification on biopsy is modeled with a pooled logistic regression model under the assumption that biopsy results are independent conditional on cancer state and covariates (age, time since diagnosis, etc.) [7, 8]. As indicated in Figure 1(a), PSA and biopsy results are also assumed to be conditionally independent given latent class.

The model depicted in Figure 1(a) is related to previous work by Lin et al. (2002), who proposed a joint latent class model (JLCM) to analyze longitudinal PSA and time-to-diagnosis of prostate cancer, extending earlier joint models by Schluchter (1992), DeGruttola and Tu (1994), and Henderson et al. (2000). Inoue et al. (2008) used a Bayesian approach to joint modeling of PSA and time-to-diagnosis at various stages of disease to estimate the underlying natural history process for prostate cancer initiation and progres-

sion. Proust-Lima and Taylor (2009) developed a dynamic extension of JLCM to predict prostate cancer recurrence after radiation therapy.

To find a credible statistical solution to the active surveillance problem requires three extensions of existing latent variable models for multivariate outcomes like the JLCM. First, the model must accommodate measurement error inherent in monitoring disease state. Second, the model must allow detection of disease state to depend on possibly informative observation times. In the JLCM of Lin et al. (2002), time-to-diagnosis is modeled as a right-censored survival outcome that, conditional on latent class, is independent of PSA. Our method models reclassification with a pooled logistic regression model [7, 8], with the possibility of reclassification conditional on the occurrence of a biopsy in each time interval. Our approach also includes a regression model for the probability of receiving a biopsy in each interval; the occurrence of a biopsy (but not its result) is allowed to depend on previous biopsy or PSA observations.

Third, the active surveillance model must allow the occurrence of a biopsy and surgical removal of the prostate to possibly be informative of the underlying cancer state. Consider the dotted lines in the DAG in Figure 1(b). If an individual's true cancer state is associated with his choice to perform a biopsy or undergo surgery after conditioning on observed PSA and biopsy results, then informative missingness is present and predictions of the cancer state that ignore it will be biased [29]. We propose including the latent cancer state as a predictor in regression models for the probability of having a biopsy and of having surgery at each time interval. In this way, the dependence between observing the outcome and its value is accommodated. This approach is comparable to the latent class dropout model proposed by Roy (2003, 2007), a type of shared parameter model with discrete random effects [13]. Unlike Roy's model for intermittent missingness which models latent class conditional on the observation process, our approach is more similar to the model

formulation outlined in Albert and Follmann (1995), as we specify distributions for the outcome and the observation process conditional on latent cancer state.

This paper is organized as follows. In Section 2, a hierarchical model for latent class prediction is described and estimation procedures are outlined. In Section 3, we specify our model to predict latent class for patients in the Johns Hopkins Active Surveillance cohort. Results of this application are presented in Section 4. We close with a discussion.

2 Hierarchical Latent Class Model

We propose a Bayesian hierarchical model of the underlying cancer state, measurement process, and clinical outcomes of patients enrolled in active surveillance (AS). Predictions are made by incorporating information from repeated PSA and biopsy measurements for all individuals with true cancer state observed in a potentially non-random subset of the cohort. Predictions are also informed by the presence of some observations, which we refer to as an *informative observation process* (IOP). In this section, we introduce notation and conditional distributions for the observed data given the latent variables and parameters, then give the likelihood function. The model is completed by specifying appropriate priors and defining the joint posterior distribution. Overall model structure is summarized in Figure 2.

2.1 Latent cancer state η_i for patient i , $i = 1, \dots, n$

Define individual i 's true cancer state, η_i , as either indolent, $\eta_i = 0$, or aggressive, $\eta_i = 1$, $i = 1, \dots, n$. We use the Gleason score that would be assigned if his entire prostate were to be surgically removed and analyzed to define $\eta_i = 0$ if Gleason = 6 and $\eta_i = 1$ if Gleason ≥ 7 . Note that this definition assumes that cancer state is constant during the time under

consideration. Relaxation of this assumption is discussed in more detail in Section 5.

True cancer state is then modeled as a Bernoulli random variable, $\eta_i \sim \text{Bern}(\rho_i)$. We assume a shared underlying probability of aggressive cancer, $\rho_i = \rho$, for simplicity in initial presentation. We observe this true cancer state on a possibly non-random subset of patients who choose surgical removal of the prostate and, hence, η_i is referred to as a “partially-latent variable”. We index patients such that $i = 1, \dots, n_{S=0}$ refers to patients without surgery ($S = 0$) and for whom η_i is latent and $i = n_{S=0} + 1, \dots, n$ refers to patients with eventual surgery and observation of η_i .

2.2 Longitudinal data Y_{im} given latent class η_i , $m = 1, \dots, M_i$

Next, we consider PSA, which is influenced by the true cancer state η_i as well as covariates including age and prostate volume. Unlike biopsies, PSA measurements are a routine part of each clinic visit so the times of observation are assumed to be independent of η_i . We use a multilevel model to estimate the linear trend (on a log scale) of an individual’s PSA as he ages [15]. Patient-level coefficients vary about an η_i -specific mean intercept and slope. Specification follows that of a hierarchically-centered multilevel model to speed convergence of the posterior sampling algorithm [14]. Specifically, given patient-level coefficients \mathbf{b}_i , the log-transformed PSA for patient i ’s m th visit, Y_{im} , is assumed equal to

$$Y_{im} = \mathbf{X}_{im}\boldsymbol{\beta} + \mathbf{Z}_{im}\mathbf{b}_i + \epsilon_{im} \tag{1}$$

where \mathbf{X}_{im} and \mathbf{Z}_{im} are covariate vectors for individual i at visit m , $\boldsymbol{\beta}$ is a parameter vector of population-level coefficients, and residual ϵ_{im} is assumed to follow a Gaussian distribution with mean zero and variance σ^2 . In comparison to the classical mixed effects model of Laird and Ware (1982), covariates in \mathbf{Z}_{im} are not a subset of covariates in \mathbf{X}_{im} ; covariates corresponding to patient-level effects, \mathbf{b}_i , are only included in \mathbf{Z}_{im} and random

effects are not centered at zero. In our application, \mathbf{Z}_{im} includes an intercept and age so that PSA intercepts and slopes vary across individuals. \mathbf{X}_{im} includes prostate volume and β is the population-level association between prostate volume and log-transformed PSA.

Modeling of patient-level coefficients follows the recommendation of Gelman and Hill (2006) who advocate the use of a scaled inverse Wishart prior on the covariance matrix. The inverse Wishart prior, which is commonly used for Bayesian estimation of multilevel models [14], imposes dependence between variance and correlation components of the covariance. To reduce prior dependence and allow for a flat prior on the correlation between individual-level intercepts and slopes, O’Malley and Zaslavsky (2008) introduce a scale parameter, ξ , for the patient-level random effects: $\mathbf{b}_i = \text{diag}(\tilde{\mathbf{b}}_i \xi^T)$. Unscaled random effects, $\tilde{\mathbf{b}}_i$, are assumed to follow a latent-class specific multivariate Gaussian distribution with mean vector $\boldsymbol{\mu}_k$ and covariance matrix Σ_k .

2.3 Biopsy Occurrence B_{ij} and Result R_{ij} for patient i in time interval j , $j = 1, \dots, J_i$

We then consider information about the true cancer state contained in the occurrence and results of prostate biopsies. Biopsy data are categorized into discrete time intervals with (B_{ij}, R_{ij}) denoting binary outcomes for individual i in time interval j indicating whether a biopsy was performed ($B_{ij} = 1$) or not ($B_{ij} = 0$) and, when it was performed, if grade reclassification occurred ($R_{ij} = 1$) or not ($R_{ij} = 0$). B_{ij} and R_{ij} are defined for $j = 1, \dots, J_i$, where J_i is the time interval of reclassification or censoring for patient i . For each time interval, we use logistic regression to model the occurrence of a biopsy and, when a biopsy

was performed, its result conditional on true cancer state:

$$\text{logit}\{P(B_{ij} = 1|\eta_i, \mathbf{U}_{ij}, \boldsymbol{\nu})\} = \mathbf{U}_{ij}\boldsymbol{\nu}_1 + \eta_i\boldsymbol{\nu}_2 + \mathbf{U}_{ij}\eta_i\boldsymbol{\nu}_3 \quad (2)$$

$$\text{logit}\{P(R_{ij} = 1|\eta_i, \mathbf{V}_{ij}, B_{ij} = 1, \boldsymbol{\gamma})\} = \mathbf{V}_{ij}\boldsymbol{\gamma}_1 + \eta_i\boldsymbol{\gamma}_2 + \mathbf{V}_{ij}\eta_i\boldsymbol{\gamma}_3 \quad (3)$$

where \mathbf{U}_{ij} and \mathbf{V}_{ij} are vectors including time-varying predictors and $\boldsymbol{\nu} = (\boldsymbol{\nu}_1, \boldsymbol{\nu}_2, \boldsymbol{\nu}_3)$ and $\boldsymbol{\gamma} = (\boldsymbol{\gamma}_1, \boldsymbol{\gamma}_2, \boldsymbol{\gamma}_3)$ are parameter vectors to be estimated that include the main effects of covariates \mathbf{U}_{ij} or \mathbf{V}_{ij} , η_i , and the possible interactions $\mathbf{U}_{ij}\eta_i$ and $\mathbf{V}_{ij}\eta_i$. Since biopsy reclassification occurs at most once, Equation 3 corresponds to a modified pooled logistic regression model for time-to-reclassification in which only intervals with biopsies performed contribute.

This model specification represents three important aspects of data generated in active surveillance: whether a biopsy is performed may be informative of true cancer state, time-to-reclassification depends on a patient's decision to receive a biopsy, and biopsy outcomes are prone to measurement error. In our application, the covariates contained in \mathbf{U}_{ij} and \mathbf{V}_{ij} may include age, time since diagnosis, and calendar date. The number of previous biopsies and recent PSA observations are also considered as predictors of B_{ij} . We do not use an interaction between true cancer state and covariates in either regression model.

2.4 Surgical Removal of Prostate S_{ij} and its Cancer Lethality η_i

Lastly, to allow for the possibility that surgical removal of the prostate, and subsequent observation of the true cancer state, is informative, we define S_{ij} to be a binary indicator of surgery ($S_{ij} = 1$) or not ($S_{ij} = 0$) for individual i during time interval j for $j = 1, \dots, J_{S_i}$, where J_{S_i} is the time of surgery or other censoring for patient i and $J_{S_i} \geq J_i$ for all i . The probability of surgery in each time interval is defined by:

$$\text{logit}(P(S_{ij} = 1|\eta_i, \mathbf{W}_{ij}, \boldsymbol{\omega})) = \mathbf{W}_{ij}\boldsymbol{\omega}_1 + \eta_i\boldsymbol{\omega}_2 + \mathbf{W}_{ij}\eta_i\boldsymbol{\omega}_3 \quad (4)$$

where \mathbf{W}_{ij} is a vector of time-varying predictors and cancer state and $\boldsymbol{\omega} = (\boldsymbol{\omega}_1, \boldsymbol{\omega}_2, \boldsymbol{\omega}_3)$ is a parameter vector to be estimated. Age, time since diagnosis, calendar date, the results of previous biopsies, and PSA are used to predict surgery. In this application, we also include an interaction between earlier grade reclassification and true state.

2.5 Posterior Distribution Estimation

Having specified models for each information source, we define the likelihood of the latent states, patient-level coefficients, and parameters given the observed data as the product of the contribution of each component described above:

$$\begin{aligned}
& L\left(\rho, \boldsymbol{\beta}, \boldsymbol{\xi}, \sigma^2, \boldsymbol{\nu}, \boldsymbol{\gamma}, \boldsymbol{\omega}; (\boldsymbol{\mu}_k, \Sigma_k), k = 0, 1; \check{\mathbf{b}}_i, i = 1, \dots, n; \eta_i, i = 1, \dots, n_{S=0} \mid \right. \\
& \quad \left. \eta_i, i = n_{S=0} + 1, \dots, n; (\mathbf{Y}_i, \underline{\mathbf{X}}_i, \underline{\mathbf{Z}}_i), (\mathbf{B}_i, \underline{\mathbf{U}}_i), (\mathbf{R}_i, \underline{\mathbf{V}}_i), (\mathbf{S}_i, \underline{\mathbf{W}}_i), i = 1, \dots, n\right) \\
& = \prod_{i=1}^n \rho^{\eta_i} (1 - \rho)^{1-\eta_i} f(\mathbf{Y}_i \mid \underline{\mathbf{X}}_i, \underline{\mathbf{Z}}_i, \boldsymbol{\beta}, \boldsymbol{\xi}, \check{\mathbf{b}}_i, \sigma^2) g(\check{\mathbf{b}}_i \mid \boldsymbol{\mu}_{\eta_i}, \Sigma_{\eta_i}) \\
& \quad \prod_{j=1}^{J_i} P(B_{ij} = 1 \mid \eta_i, \mathbf{U}_{ij}, \boldsymbol{\nu})^{B_{ij}} P(B_{ij} = 0 \mid \eta_i, \mathbf{U}_{ij}, \boldsymbol{\nu})^{1-B_{ij}} \\
& \quad \quad (P(R_{ij} = 1 \mid \eta_i, \mathbf{V}_{ij}, \boldsymbol{\gamma})^{R_{ij}} P(R_{ij} = 0 \mid \eta_i, \mathbf{V}_{ij}, \boldsymbol{\gamma})^{1-R_{ij}})^{B_{ij}} \\
& \quad \prod_{j=1}^{J_{S_i}} P(S_{ij} = 1 \mid \eta_i, \mathbf{W}_{ij}, \boldsymbol{\omega})^{S_{ij}} P(S_{ij} = 0 \mid \eta_i, \mathbf{W}_{ij}, \boldsymbol{\omega})^{1-S_{ij}}. \tag{5}
\end{aligned}$$

where f and g are multivariate normal densities for the vector of log-transformed PSAs \mathbf{Y}_i and unscaled random effects $\check{\mathbf{b}}_i$, respectively, each with mean and covariance as defined above. $\underline{\mathbf{X}}_i$ denotes the matrix of covariate vectors $[\mathbf{X}_{i1}, \dots, \mathbf{X}_{iM_i}]$; $\underline{\mathbf{Z}}_i$, $\underline{\mathbf{U}}_i$, $\underline{\mathbf{V}}_i$, and $\underline{\mathbf{W}}_i$ are similarly defined. \mathbf{B}_i , \mathbf{R}_i , and \mathbf{S}_i denote vectors of all biopsy, reclassification, and surgery observations for individual i .

We use a Bayesian approach to estimate the joint posterior distribution of parameters,

latent states, and patient-level coefficients given the observed data. The prior distributions for the latent states and random effects have been described (Sections 2.1 and 2.2, respectively). Standard prior distributions are used for model parameters including a beta prior on the probability of having aggressive cancer (ρ) and minimally informative Gaussian priors on logistic regression model coefficients, as shown in Figure 2. .

The joint posterior distribution of the parameters, latent states, and random effects can now be written:

$$\begin{aligned}
& p\left(\rho, \boldsymbol{\beta}, \xi, \sigma^2, \boldsymbol{\nu}, \boldsymbol{\gamma}, \boldsymbol{\omega}; (\boldsymbol{\mu}_k, \boldsymbol{\Sigma}_k); \check{\mathbf{b}}_i, i = 1, \dots, n; \eta_i, i = 1, \dots, n_{S=0} \mid \right. \\
& \quad \left. \eta_i, i = n_{S=0} + 1, \dots, n; (\mathbf{Y}_i, \mathbf{X}_i, \mathbf{Z}_i), (\mathbf{B}_i, \mathbf{U}_i), (\mathbf{R}_i, \mathbf{V}_i), (\mathbf{S}_i, \mathbf{W}_i), i = 1, \dots, n; \boldsymbol{\Theta}\right) \\
& \propto L\left(\rho, \boldsymbol{\beta}, \xi, \sigma^2, \boldsymbol{\nu}, \boldsymbol{\gamma}, \boldsymbol{\omega}; (\boldsymbol{\mu}_k, \boldsymbol{\Sigma}_k); \check{\mathbf{b}}_i, i = 1, \dots, n; \eta_i, i = 1, \dots, n_{S=0} \mid \right. \\
& \quad \left. \eta_i, i = n_{S=0} + 1, \dots, n; (\mathbf{Y}_i, \mathbf{X}_i, \mathbf{Z}_i), (\mathbf{B}_i, \mathbf{U}_i), (\mathbf{R}_i, \mathbf{V}_i), (\mathbf{S}_i, \mathbf{W}_i), i = 1, \dots, n\right) \\
& \quad \times \boldsymbol{\pi}\left(\rho, \boldsymbol{\beta}, \xi, \sigma^2, \boldsymbol{\nu}, \boldsymbol{\gamma}, \boldsymbol{\omega}; (\boldsymbol{\mu}_k, \boldsymbol{\Sigma}_k) \mid \boldsymbol{\Theta}\right) \tag{6}
\end{aligned}$$

where $\boldsymbol{\pi}(\cdot \mid \boldsymbol{\Theta})$ denotes the joint prior density for model parameters with hyperparameters $\boldsymbol{\Theta}$ and indexing on j and k suppressed for clarity in presentation.

For those patients without η_i observed, the true unobserved cancer state is sampled from its full conditional posterior at each iteration of the MCMC sampling algorithm. Averaging the resulting posterior sample produces the posterior probability that a patient has a true Gleason 7 or higher prostate cancer ($\eta_i = 1$). These posterior predictions can then be communicated to clinicians and patients to inform decision-making. Posterior estimates of PSA trajectory and risk of grade reclassification on a subsequent biopsy can also be summarized and included in any decision support tool.

3 Johns Hopkins Active Surveillance Cohort

3.1 The Data

From January 1995 to June 2014, the Johns Hopkins Active Surveillance cohort has enrolled 1,298 prostate cancer patients [43]. This study prospectively follows patients with very-low-risk or low-risk prostate cancer diagnoses (according to criteria outlined in Epstein et al. (1994)) who elect to delay curative intervention in favor of active surveillance (AS). Characteristics of diagnostic biopsies and results of all prior PSA tests are collected at enrollment. As part of the surveillance regimen, PSA tests are typically performed every six months and biopsies are performed annually, though these intervals vary based upon patient preferences and clinician recommendations. Treatment, including surgery and radiation, is recommended upon biopsy grade reclassification, that is, when the Gleason score assigned on a biopsy first exceeds 6. Some patients also choose to undergo treatment prior to reclassification. For all patients who elect surgical removal of the prostate, the true Gleason for the entire prostate is also recorded.

A total of 874 patients who met study criteria and had at least two PSA measurements and at least one post-diagnosis biopsy as of October 1, 2014 were included in the analysis. Patients still active in the program were administratively censored at this date. Otherwise, observations on a patient were censored when he received treatment, died, or was lost to follow-up. Loss to follow-up was defined as two years without a PSA or biopsy after the most recent observation. The number of observations and years of follow-up available for analysis are summarized in Table 1. 318 patients (36%) were censored due to receiving some treatment, 130 (15%) were lost to follow-up, and 19 (2.2%) were censored due to death. (No patients died of prostate cancer.) 407 patients (47%) remained active in the program at the time of data collection.

	Total # observations	Median # per patient (IQR)
PSA	10,425	10 (6,16)
Biopsy	2,741	3 (1,4)
Years of follow-up (prior to reclassification)	4,980	5 (3,8)

Table 1: Summary of observations and follow-up time for $n=874$ patients included in analysis.

Grade reclassification was observed in 160 patients (18%). 167 patients (19%) elected surgical removal of the prostate; 78 had a prior reclassification. 161 patients had a definitive post-surgical Gleason score determination. Results of the biopsy-based estimated Gleason score and post-surgical true value are shown in Table 2. Nearly a third of patients with final biopsy Gleason scores of 6 were found upon prostatectomy to have Gleason 7 or higher grade prostate cancer while a quarter of those with grade reclassification observed on biopsy were downgraded after surgery.

3.2 Model Specification

We applied models with and without the informative observation process (IOP) components (occurrence of biopsy and surgery) to data from the Johns Hopkins Active Surveillance cohort.

PSA trajectory was modeled with a hierarchically-centered multilevel model, as described in Section 2. Patient-level coefficients for intercept and age were estimated for each patient. A shared covariance matrix was assumed for the unscaled random effects, that is

		Biopsy Gleason Score		
		6	≥ 7	Total
Post-surgical True Value	Indolent, $\eta = 0$	66 (69%)	17 (26%)	83
	Aggressive, $\eta = 1$	30 (31%)	48 (74%)	78
Total		96	65	161

Table 2: Summary of post-surgical cancer state determination (η) compared to final biopsy-based Gleason score (with column percentages).

$\Sigma_0 = \text{Var}(\check{\mathbf{b}}_i | \eta_i = 0) = \text{Var}(\check{\mathbf{b}}_i | \eta_i = 1) = \Sigma_1$, in order to aid identifiability. The plausibility of this assumption was checked by examining these estimated covariance matrices in the subset of patients with known cancer state. The PSA model also included a population-level coefficient for prostate volume, which was measured via ultrasound at some biopsies. Since changes in prostate volume due to age and cancer activity are expected to be of a smaller magnitude than the measurement error in ultrasound-guided volume assessment, the average of available prostate volume observations was used for each patient.

The Johns Hopkins' AS protocol is to perform a biopsy once per year. Hence, biopsy, reclassification, and surgery observations were categorized into annual intervals. A small number (1%) of intervals contained two biopsies. To accommodate this, we redefine the logistic regression model in Equation (2) as the probability of any biopsies during the year. Intervals with two biopsies then contributed two conditionally independent reclassification outcomes (Equation 3) to the likelihood.

Exploratory data analysis was performed to identify predictors of biopsy, reclassification, and surgery. For each of the three outcomes, covariates were selected that lowered

the Akaike Information Criterion (AIC) of a multivariable logistic regression model for that outcome [1]. Natural splines with up to four degrees of freedom and knots at percentiles of the predictor variable were used when doing so lowered the AIC. True cancer state, age, time since diagnosis, and calendar time were included as predictors for all outcomes. The number of previous biopsies was included as a predictor of biopsy and surgery as well. The regression model for surgery also included previous biopsy results– grade reclassification, number of positive cores sampled and maximum percent involvement of any core.

Model parameters and their minimally informative priors are presented in the model summary given in Figure 2. Posterior sampling was performed in R2JAGS with code available at <http://github.com/rycoley/prediction-prostate-surveillance>. Simulated data is also provided. Regulations on patient privacy prohibit us from showing or sharing actual clinical data. Data were generated using posterior estimates of model parameters and summary measures of relevant baseline covariate data for JHAS patients

3.3 Model Assessment

Predictive accuracy was assessed in two ways. For patients with true cancer state observed, leave-one-out cross validation was used to obtain posterior distributions of η_i . These out-of-sample predictions of η_i were then compared to known values with receiver operating characteristic (ROC) curves [19] and calibration plots [42]. For the former, the area under the curve (AUC) and associated 95% bootstrapped confidence interval were calculated [22]. For the latter, a plot comparing posterior predictions to observed rates of class membership was constructed by performing logistic regression of the observed true state on a natural spline representation of out-of-sample posterior predictions (degrees of freedom = 2).

Calibration plots were also drawn to assess model fit for outcomes observed on all patients: the occurrence of a biopsy, grade reclassification on biopsy, and the occurrence

	Cancer State	PSA	Biopsy	Surgery
<u>Data</u>	Outcome Covariates	η_i $Y_{im}, m = 1, \dots, M_i$ $(\mathbf{X}_{im}, \mathbf{Z}_{im}), m = 1, \dots, M_i$	$(B_{ij}, R_{ij}), j = 1, \dots, J_i$ $(\mathbf{U}_{ij}, \mathbf{V}_{ij}), j = 1, \dots, J_i$	$S_{ij}, j = 1, \dots, J_{S_i}$ $\mathbf{W}_{ij}, j = 1, \dots, J_{S_i}$
<u>Model</u>	$\eta_i \sim \text{Bern}(\rho)$	$\tilde{\mathbf{b}}_i \eta_i = k \sim \text{MVN}(\boldsymbol{\mu}_k, \Sigma)$ $\mathbf{b}_i = \text{diag}(\tilde{\mathbf{b}}_i \boldsymbol{\xi}^T)$ $Y_{im} \sim N(\mathbf{X}_{im} \boldsymbol{\beta} + \mathbf{Z}_{im} \mathbf{b}_i, \sigma^2)$	$B_{ij} \eta_i, \mathbf{U}_{ij} \sim \text{Bern}(P(B_{ij} = 1 \eta_i, \mathbf{U}_{ij}, \boldsymbol{\nu}))$ $R_{ij} \eta_i, \mathbf{V}_{ij} \sim \text{Bern}(P(R_{ij} = 1 \eta_i, \mathbf{V}_{ij}, \boldsymbol{\gamma}))$	$S_{ij} \eta_i, \mathbf{W}_{ij} \sim \text{Bern}(P(S_{ij} = 1 \eta_i, \mathbf{W}_{ij}, \boldsymbol{\omega}))$
<u>Priors</u>	$\rho \sim \text{Beta}(1, 1)$	$\boldsymbol{\mu}_k \sim \text{MVN}(\mathbf{0}, 10^2 \times \mathbf{I}_{D_Z}), k = 0, 1$ $\Sigma \sim \text{InvWish}(\mathbf{I}_{D_Z}, D_Z + 1)$ $\xi_d \sim U(0, 10), d = 1, \dots, D_Z$ $\boldsymbol{\beta} \sim \text{MVN}(\mathbf{0}, 10^2 \times \mathbf{I}_{D_X})$ $\sigma^2 \sim U(0, 10)$	$\boldsymbol{\nu} \sim \text{MVN}(\mathbf{0}, 10^2 \times \mathbf{I}_{D_U})$ $\boldsymbol{\gamma} \sim \text{MVN}(\mathbf{0}, 10^2 \times \mathbf{I}_{D_V})$	$\boldsymbol{\omega} \sim \text{MVN}(\mathbf{0}, 10^2 \times \mathbf{I}_{D_W})$

Figure 2: Model summary with priors used for application to Johns Hopkins Active Surveillance data. D_X is the length of vector \mathbf{X} and \mathbf{I}_{D_X} is the identity matrix with dimension D_X . D_Z , D_U , D_V , and D_W and the associated identity matrices are similarly defined for covariates vectors Z , U , V , and W .

of surgery. Observed binary outcomes were regressed on a natural spline representation of the posterior probabilities of the event in each person-year for every saved iteration of the posterior sampling algorithm. Code for reproducing all plots is available at <http://github.com/rycoley/prediction-prostate-surveillance>.

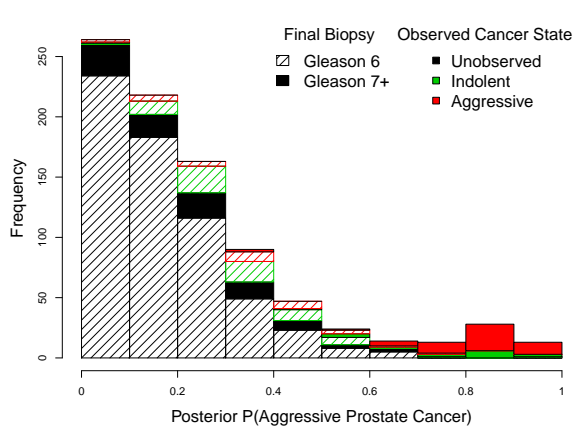
4 Results

Posterior predictions of η were obtained for all patients in the dataset, including out-of-sample predictions for patients who underwent surgery. A histogram of predictions of η from the model with IOP components is given in Figure 3(a). In this stacked histogram, bar colors indicate whether η was observed and, if so, its value. Diagonal shading represents patients whose final biopsy was assigned a Gleason score of 6 while solid bars represent

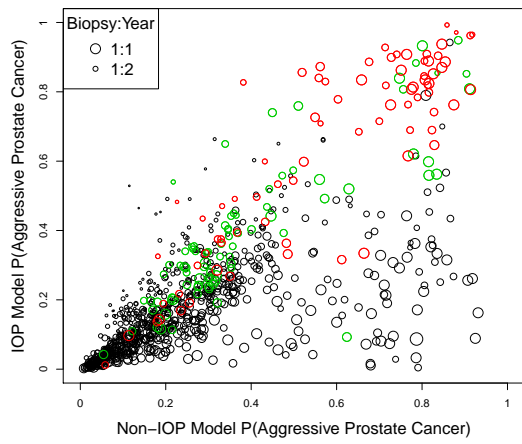
patients whose final biopsy was assigned a Gleason score of 7 or higher (i.e., grade reclassification). Patients with posterior predictions above 60% are primarily those who both experienced grade reclassification and elected prostatectomy. 95% of AS patients who neither reclassified nor underwent surgery have posterior predictions that are lower than 50%; a majority have predictions below 20%.

Figure 3(b) shows a scatterplot comparing posterior probabilities of aggressive cancer, $P(\eta = 1)$, between models with and without IOP components. The color of plotting symbols represents observation of the true cancer state, and symbol size is an indication of the frequency with which a patient received prostate biopsies; larger circles represent more frequent biopsies while smaller circles represent less frequent biopsies. In this scatterplot, we see that the models with and without IOP components produce similar posterior predictions for most patients, particularly those patients for which the non-IOP model assigns very low risk. Inclusion of IOP components decreases posterior predictions of η most markedly for patients with frequent biopsies and no surgery (larger black circles below the $x=y$ axis) and tends to increase posterior predictions for patients who elect surgery or have infrequent biopsies (colored or smaller black circles, respectively, above the $x=y$ axis).

Posterior predictions of η from the proposed IOP model are estimated to be more accurate than both predictions from the model without IOP components and using a patient’s last biopsy result as a predictor for true cancer state, as illustrated by the ROC curves in Figure 4(a). The out-of-sample AUC among patients with observed true cancer state is 0.75 (95% CI: 0.67, 0.83) for the model incorporating IOP components, slightly higher than the non-IOP model which has an AUC of 0.72 (0.64, 0.81). We can also compare the specificity of each model’s predictions to that of the binary classifier defined by final biopsy result. Final biopsy result predicts true cancer state with a sensitivity of 62% (50, 72%) and specificity of 80% (71, 88%) (see Table 2). Fixing sensitivity at 62%, we see



(a) Histogram of IOP predictions

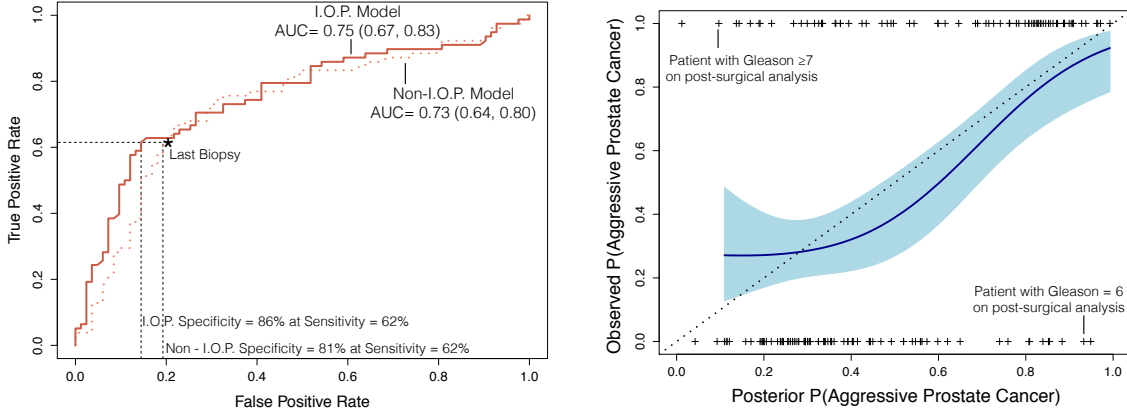


(b) IOP vs Non-IOP predictions

Figure 3: Posterior predictions of true prostate cancer state. Coloring indicates the whether η was observed and, if so, its value.

that the IOP predictions have a specificity of 86% (77, 93%) and non-IOP predictions have a specificity of 81% (71, 89%). The improvement in specificity offered by the IOP model corresponds to avoiding, on average, 1 in 4 unnecessary diagnoses of more aggressive cancer in comparison to a diagnosis based solely on a patient’s most recent biopsy (-1 in 2.5, 1 in 1.5).

Posterior predictions of η from the IOP model also appear to accurately estimate a patient’s risk of having more aggressive cancer. The calibration plot in Figure 4(b) shows that, for patients with known values of η , the average observed value of η is close to the average posterior predicted probability of $\eta = 1$, indicating that the model reasonably reproduces the mean of observations. In this plot, hashmarks at $y=0$ and $y=1$ correspond to observed cancer states ($\eta = 0, 1$, respectively) plotted at their posterior probability of the true state on the x-axis. Shading shows the 95% point-wise confidence interval around



(a) ROC curves, IOP and non-IOP predictions (b) Calibration plot for IOP predictions

Figure 4: Predictive accuracy of out-of-sample predictions of η among those with true state observed. In (a), the specificity of predictions from each model is highlighted at the sensitivity of a binary classifier defined by final biopsy result (*). In (b), the dark line shows the empirical rate of observing a true Gleason score of 7 or above (y-axis) given an out-of-sample posterior probability of true state (x-axis) under the model with IOP components; shading gives the 95% point-wise confidence interval. Perfect agreement lies on the $x=y$ axis (dotted line).

the fitted values (dark line) from a logistic regression of the observed states on a natural spline function of the out-of-sample posterior probabilities.

The risks of clinical outcomes (biopsy results) and choices (occurrence of biopsy and surgery) for all patients appear to be accurately estimated by the IOP model as well, as demonstrated by calibration plots in Figure 5. Solid lines show, for each saved iteration of the sampling chain, the fitted values of a logistic regression of the observed outcome on the natural spline representation of each person-year’s posterior probability of an event.

Plotting symbols at $y=0$ and $y=1$ correspond to the observed outcome and are plotted on the x-axis at the mean posterior probability for that person-year; plotting symbol shape and color indicate eventual observations of the true state. Posterior probabilities and observed rates are generally similar to each other, with closer agreement occurring in ranges with more data.

The goal of this modeling approach is to provide individual patients with predictions of their true cancer state in order to support clinical decision making. Plots in Figure 6 show posterior predictions of η from the IOP model as well as predictions of future PSA and biopsy values for a dozen patients. For each patient, plotting circles represent simulated PSA observations, with the scale given on the lefthand y-axis. Triangles represent simulated biopsies, with open triangles indicating no biopsy in an annual interval (and, thus, no reclassification observed) and filled triangles indicating biopsy results: triangles at the bottom of the plot represent a Gleason score of 6 while those at the top represent a Gleason score of 7 or higher on biopsy. Posterior predictions of each patient's η value are given above the plot. Shaded 95% credible intervals indicate the likely PSA trajectory and risk of reclassification on a future biopsy ($P(R = 1|\text{data})$, scale on righthand axis) for each patient. The darkest shading occurs at the center of the posterior distribution (47.5-52.5 percentile) and progressively lighter shading is used at every posterior decile (42.5-57.5, . . . , 2.5-97.5 percentiles). Note that no reclassification projection is given for the patient with an observed Gleason score of 7 or higher on biopsy. Since biopsy outcomes are censored at the time of grade reclassification, post-reclassification predictions are not valid.

4.1 Identifiability of IOP components

The posterior distributions of IOP coefficients, i.e., the effect of η on biopsy occurrence and surgery, indicate that the data contain evidence of informative missingness, as shown

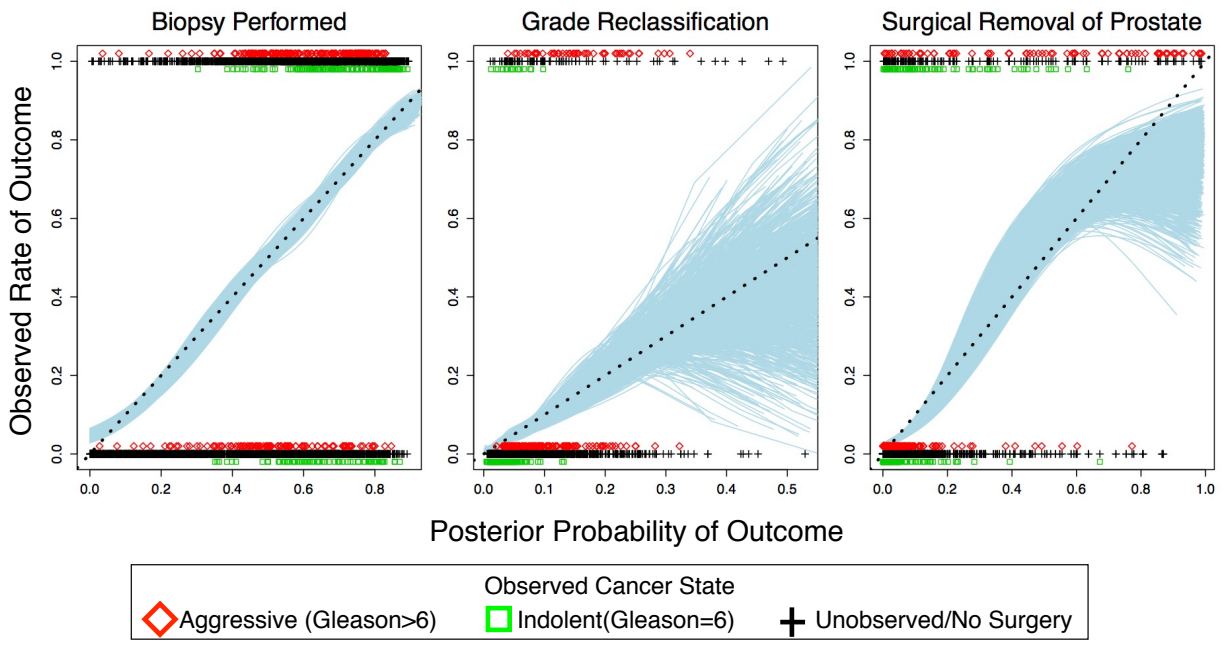


Figure 5: Calibration plots for predictions of the occurrence of a biopsy (left), grade reclassification (center), and surgery (right) at annual intervals for all patients. Each solid line represents agreement between the posterior probability and observed event rate for a single iteration of the sampling algorithm.

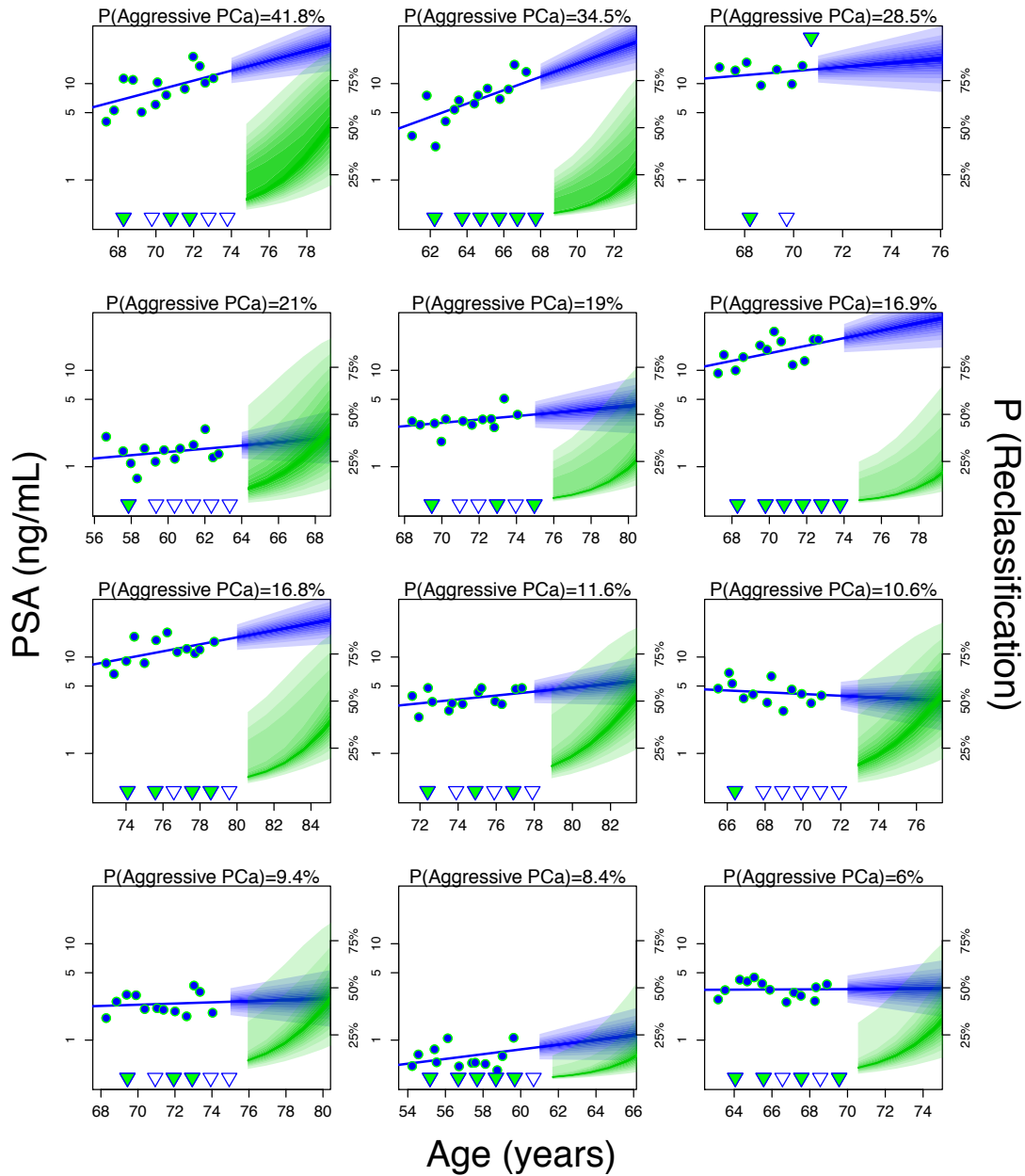


Figure 6: Simulated PSA (circles) and reclassification (triangle) data for a dozen patients. Vertical position of filled triangles indicate results of biopsies received— triangles at the bottom represent Gleason 6 observations while those on top represent Gleason 7 or above; open triangles indicate missed biopsies. Posterior probabilities of having aggressive prostate cancer (PCa) are shown above each patient’s data. Shaded intervals show posterior credible intervals around projected PSA and reclassification trajectories with shading gradations indicating deciles of the interval and darkest shading occurring at the posterior median.

in Figure 7 (bold, solid lines in each plot). 95% quantile-based credible intervals of the log-odds ratio (OR) for the effect of $\eta = 1$ on the probability of having a biopsy in an interval (lefthand plot) and the log-OR for the interaction between $\eta = 1$ and prior grade reclassification (righthand plot) exclude 0 (vertical line).

An important question is whether the additional parameters in the IOP model, especially those associated with observation of the true cancer state, are well-identified by the likelihood function for the available data. To assess robustness of posterior predictions to prior specification, we refit the IOP model with multiple informative priors on both the log-OR of surgery given true state and the log-OR of surgery given an interaction between true state and prior biopsy results. Specifically, we considered all combinations of normal priors with a variance of one and mean OR of one-half, one, and two for the association of η_i and $\eta_i \times \mathbf{1}_{[R_{i\bar{j}}=1]}$ with the probability of surgery for patient i in year j (where $\mathbf{1}_{[R_{i\bar{j}}=1]}$ is an indicator of grade reclassification for patient i during or prior to year j). The resulting posterior distributions, shown in Figure 7, demonstrate relative robustness to prior specification and affirm confidence in posterior predictions from the IOP model with vague priors. The primary effects of specifying these more informative priors appear to be a reduction in the variability of posterior distributions and an attenuation of the estimated effect of the interaction of $\eta = 1$ and prior grade reclassification on the risk of surgery. Posterior predictions of η and the model's predictive accuracy were not changed by specifying informative priors on IOP components (not shown). It appears that repeated contributions to the likelihood of the probability of not having surgery ($P(S_{ij} = 0)$) in intervals prior to the decision to have surgery provide enough information on the relationship between the true cancer state and its eventual observation for this relationship to be identifiable.

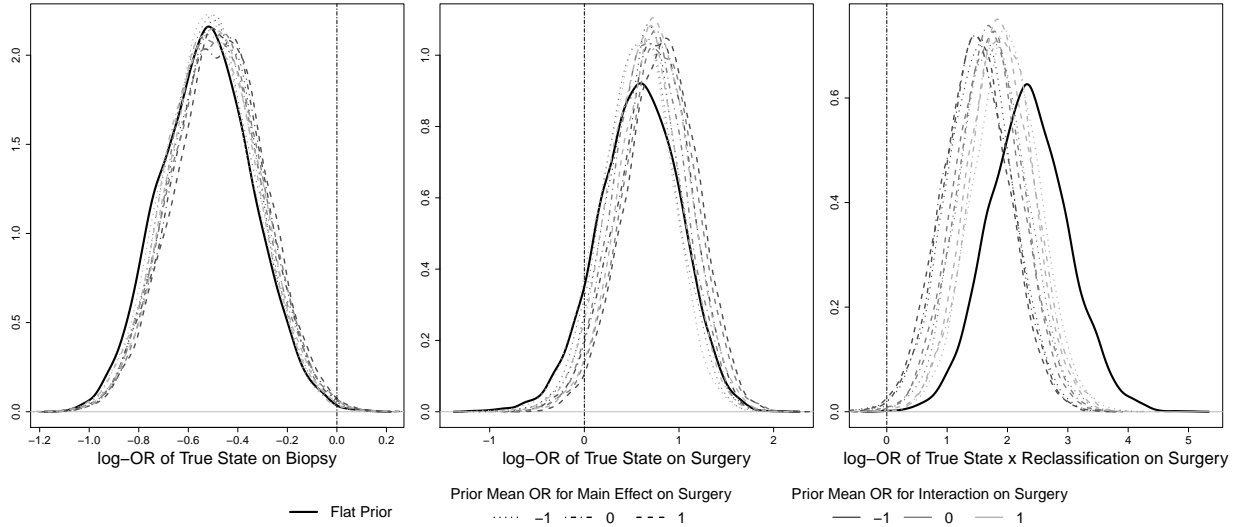


Figure 7: Posterior distributions for IOP coefficients under vague and informative priors.

5 Discussion

In this paper, we have presented a hierarchical Bayesian model for predicting latent cancer state among low risk prostate cancer patients. Multiple models have been developed to predict biopsy results in this population [3, 45]. However, our model predicts the outcome of chief interest—the true underlying state of an individual’s prostate cancer. Focusing on the actual health state, even when latent, is equivalent to subsetting patients into subgroups for which optimal treatments differ. Subsetting is the goal of precision medicine [37].

The proposed model integrates four sources of information about whether a tumor is aggressive or indolent: repeated measures on the biomarker PSA; repeated results from tissue biopsies; repeated decisions to have a biopsy; and the time to surgical removal of the prostate. In the subset of patients that have their prostates removed, the true tumor pathology state is observed. This data-integrating method is an example of semi-supervised

learning [5]. Wu et al. (2015) referred to models like this as “partially-latent”.

The methods proposed here are tailored to available measurements that address the clinical questions arising from active surveillance of prostate cancer: should I have a biopsy this year; what is the chance my tumor is indolent; should I undertake removal or irradiation of my prostate despite the known serious side effects? The model extends naturally to provide improved answers to these questions as additional data become available. For example, when genetic markers for prostate cancer risk are identified, the probability distribution for latent state (ρ_i) could easily be informed by subgroups defined by their expression. Or, when MRI or ultrasound images are commonly used before biopsy, these data will be included in the model as well. In the case that some measurements are not available for all patients, the proposed framework is also able to adjust for informative observation of predictors and outcomes.

The proposed model can also be modified in response to advancement in scientific understanding about the relationship between clinical measurements and the underlying cancer state. In particular, in the event of new research findings on the rate of progression in this population, the model could be extended to allow an indolent cancer to transition to a lethal one, for example, as a Markov process. Because an individual’s true cancer state can only be observed once, the current data contain insufficient information to simultaneously support identifiability of both the rate of biopsy misclassification and the rate of pathological progression in the underlying state. The model currently assumes that an individual’s cancer categorization (Gleason score) does not change over the time period under surveillance while allowing for imperfect sensitivity and specificity of biopsies. This assumption reflects the current clinical understanding that biopsy upgrading in AS is more frequently due to misdiagnosis rather than true grade progression [32]. A more recent analysis by Inoue et al. (2014) suggests a rate of disease progression in the Johns Hopkins

AS cohort of 12-14% within a decade of enrollment, but this estimate is sensitive to prior specification. A dynamic state extension would require strong prior knowledge about the progression rate parameter in order to be identifiable from the current data. The effect of allowing for a state transition would be to give greater weight to more recent PSA and biopsy data outcomes when predicting the underlying state rather than giving equal weight to all of the observations.

The proposed prediction model exemplifies the statistical underpinnings of a learning health care system [18, 40], a system with the ability to continuously integrate patient data and medical knowledge to optimize patient care. As more patients enroll in the Johns Hopkins Active Surveillance cohort, and as more information is collected on existing patients, our ability to predict underlying health states and the likely trajectory of clinical outcomes will improve. Furthermore, importance sampling methods can be used to obtain real-time prediction updates based on the most current information in order to support decision-making in a clinical setting (see technical report [12]). An example interactive decision-support tool that provides fast predictions of a patient’s latent prostate cancer state is demonstrated at <https://rycoley.shinyapps.io/dynamic-prostate-surveillance>.

References

- [1] Hirotogu Akaike. Information theory and an extension of the maximum likelihood principle. In *Selected Papers of Hirotogu Akaike*, pages 199–213. Springer, 1998.
- [2] Paul S Albert and Dean A Follmann. Shared-parameter models. *Longitudinal data analysis*, pages 433–452, 2009.

- [3] Donna P Ankerst, Jing Xia, Ian M Thompson, Josef Hoefler, Lisa F Newcomb, James D Brooks, Peter R Carroll, William J Ellis, Martin E Gleave, Raymond S Lance, et al. Precision medicine in active surveillance for prostate cancer: Development of the canary–early detection research network active surveillance biopsy risk calculator. *European urology*, 2015.
- [4] H. Ballentine Carter, Anna Kettermann, Christopher Warlick, E. Jeffrey Metter, Patricia Landis, Patrick C. Walsh, and Jonathan I. Epstein. Expectant management of prostate cancer with curative intent: an update on the Johns Hopkins experience. *Journal of Urology*, 178:2359–2364, 2007.
- [5] Olivier Chapelle, Bernhard Schölkopf, Alexander Zien, et al. *Semi-supervised learning*. MIT press Cambridge, 2006.
- [6] Roger Chou, Jennifer M. Croswell, Dana Tracy, Christina Bougatsos, Ian Blazina, Rongwei Fu, Ken Gleitsmann, Helen C. Koenig, Clarence Lam, Ashley Maltz, J. Bruin Ruggie, and Kenneth Lin. Screening for prostate cancer: a review of the evidence for the U.S. Preventive Services Task Force. *Annals of Internal Medicine*, 155:762–771, 2011.
- [7] L Adrienne Cupples, Ralph B D’Agostino, Keaven Anderson, and William B Kannel. Comparison of baseline and repeated measure covariate techniques in the framingham heart study. *Statistics in medicine*, 7(1-2):205–218, 1988.
- [8] Ralph B D’Agostino, Mei-Ling Lee, Albert J Belanger, L Adrienne Cupples, Keaven Anderson, and William B Kannel. Relation of pooled logistic regression to time dependent cox regression analysis: the framingham heart study. *Statistics in medicine*, 9(12):1501–1515, 1990.

- [9] Victor DeGruttola and Xin Ming Tu. Modelling progression of CD4-lymphocyte count and its relationship to survival time. *Biometrics*, 50:1003–1014, 1994.
- [10] Jonathan I. Epstein, Zhaoyong Feng, Bruce J. Trock, and Phillip M. Pierorazio. Upgrading and downgrading of prostate cancer from biopsy to radical prostatectomy: Incidence and predictive factors using the modified Gleason grading system and factoring in tertiary grades. *European Urology*, 61:1019–1024, 2012.
- [11] Jonathan I. Epstein, Patrick C. Walsh, Marné Carmichael, and Charles B. Brendler. Pathologic and clinical findings to predict tumor extent of non palpable (stage T1c) prostate cancer. *Journal of the American Medical Association*, 271:368–374, 1994.
- [12] Aaron J Fisher, R Yates Coley, and Scott L Zeger. Fast out-of-sample predictions for bayesian hierarchical models of latent health states. *arXiv preprint arXiv:1510.08802*, 2015.
- [13] Dean Follmann and Margaret Wu. An approximate generalized linear model with random effects for informative missing data. *Biometrics*, pages 151–168, 1995.
- [14] Alan E Gelfand, Sujit K Sahu, and Bradley P Carlin. Efficient parametrisations for normal linear mixed models. *Biometrika*, 82(3):479–488, 1995.
- [15] Andrew Gelman and Jennifer Hill. *Data analysis using regression and multi-level/hierarchical models*. Cambridge University Press, 2006.
- [16] D.F. Gleason. The Veteran’s Administration Cooperative Urologic Research Group: Histologic grading and clinical staging of prostatic carcinoma. In M. Tannenbaum, editor, *Urologic Pathology: The Prostate*, pages 171–198. Lea and Febiger, Philadelphia, 1977.

- [17] Donald F Gleason. Histologic grading of prostate cancer: a perspective. *Human pathology*, 23(3):273–279, 1992.
- [18] WA Goolsby, L Olsen, and M McGinnis. Iom roundtable on value and science-driven health care. In *Clinical data as the basic staple of health learning: creating and protecting a public good: workshop summary*, pages 134–140, 2012.
- [19] James A Hanley and Barbara J McNeil. The meaning and use of the area under a receiver operating characteristic (roc) curve. *Radiology*, 143(1):29–36, 1982.
- [20] Erika Check Hayden. Personalized cancer therapy gets closer. *Nature News*, 458(7235):131–132, 2009.
- [21] Robin Henderson, Peter Diggle, and Angela Dobson. Joint modelling of longitudinal measurements and event time data. *Biostatistics*, 1(4):465–480, 2000.
- [22] David W Hosmer Jr, Stanley Lemeshow, and Rodney X Sturdivant. *Applied logistic regression*, volume 398. John Wiley & Sons, 2013.
- [23] Lurdes Y T Inoue, Ruth Etzioni, Christopher Morrell, and Peter Müller. Modeling disease progression with longitudinal markers. *Journal of the American Statistical Association*, 103(481):259–270, 2008.
- [24] Lurdes Y.T. Inoue, Bruce J. Trock, Alan W. Partin, Herbert B. Carter, and Ruth Etzioni. Modeling grade progression in an active surveillance study. *Statistics in Medicine*, 33:930–939, 2014.
- [25] Ali Khatami, Damber Jan-Erik, Lilja Hans, Lodding Pär, and Hugosson Jonas. Psa doubling time predicts the outcome after active surveillance in screening-detected

- prostate cancer: Results from the european randomized study of screening for prostate cancer, sweden section. *International journal of cancer*, 120(1):170–174, 2007.
- [26] L Klotz, L. Zhang, A. Lam, and et al. Clinical results of long-term follow-up of a large, active surveillance cohort with localized prostate cancer. *Journal of Clinical Oncology*, 2010:126–131, 2010.
- [27] Nan M Laird and James H Ware. Random-effects models for longitudinal data. *Biometrics*, pages 963–974, 1982.
- [28] Haiqun Lin, Bruce W Turnbull, Charles E McCulloch, and Elizabeth H Slate. Latent class models for joint analysis of longitudinal biomarker and event process data: application to longitudinal prostate-specific antigen readings and prostate cancer. *Journal of the American Statistical Association*, 97(457):53–65, 2002.
- [29] Roderick JA Little and Donald B Rubin. *Statistical analysis with missing data*. John Wiley & Sons, 2014.
- [30] Michael McGeachie, Rachel L Badovinac Ramoni, Josyf C Mychaleckyj, Karen L Furie, Jonathan M Dreyfuss, Yongmei Liu, David Herrington, Xiuqing Guo, João A Lima, Wendy Post, et al. Integrative predictive model of coronary artery calcification in atherosclerosis. *Circulation*, 120(24):2448–2454, 2009.
- [31] A James O’Malley and Alan M Zaslavsky. Domain-level covariance analysis for multilevel survey data with structured nonresponse. *Journal of the American Statistical Association*, 103(484):1405–1418, 2008.
- [32] Sima P Porten, Jared M Whitson, Janet E Cowan, Matthew R Cooperberg, Katsuto Shinohara, Nannette Perez, Kirsten L Greene, Maxwell V Meng, and Peter R

- Carroll. Changes in prostate cancer grade on serial biopsy in men undergoing active surveillance. *Journal of Clinical Oncology*, 29(20):2795–2800, 2011.
- [33] Cécile Proust-Lima and Jeremy MG Taylor. Development and validation of a dynamic prognostic tool for prostate cancer recurrence using repeated measures of posttreatment psa: a joint modeling approach. *Biostatistics*, 10(3):535–549, 2009.
- [34] Jason Roy. Modeling longitudinal data with nonignorable dropouts using a latent dropout class model. *Biometrics*, 59(4):829–836, 2003.
- [35] Jason Roy. Latent class models and their application to missing-data patterns in longitudinal studies. *Statistical methods in medical research*, 2007.
- [36] Sameer D Saini, Frank van Hees, and Sandeep Vijan. Smarter screening for cancer: possibilities and challenges of personalization. *JAMA*, 312(21):2211–2212, 2014.
- [37] Suchi Saria and Anna Goldenberg. Subtyping: What it is and its role in precision medicine. *Intelligent Systems, IEEE*, 30(4):70–75, 2015.
- [38] Mark D Schluchter. Methods for the analysis of informatively censored longitudinal data. *Statistics in medicine*, 11(14-15):1861–1870, 1992.
- [39] Peter Schulam, Fredrick Wigley, and Suchi Saria. Clustering longitudinal clinical marker trajectories from electronic health data: Applications to phenotyping and endotype discovery. In *Twenty-Ninth AAAI Conference on Artificial Intelligence*, 2015.
- [40] Mark Smith, Robert Saunders, Leigh Stuckhardt, J Michael McGinnis, et al. *Best care at lower cost: the path to continuously learning health care in America*. National Academies Press, 2013.

- [41] Mark S. Soloway, Cynthia T. Soloway, Steve Williams, Ranjinkanth Ayyathurai, Bruce Kava, and Murugesan Manoharan. Active surveillance; A reasonable management alternative for patients with prostate cancer: The Miami experience. *BJU International*, 101:165–169, 2008.
- [42] Ewout W Steyerberg, Andrew J Vickers, Nancy R Cook, Thomas Gerds, Mithat Gonen, Nancy Obuchowski, Michael J Pencina, and Michael W Kattan. Assessing the performance of prediction models: a framework for some traditional and novel measures. *Epidemiology (Cambridge, Mass.)*, 21(1):128, 2010.
- [43] Jeffrey J. Tosoian, Mufaddal Mamawala, Jonathan Epstein, Patricia Landis, Sacha Wolf, Bruce J. Tock, and H. Ballentine Cater. Immediate and longer term outcomes for a prospective active surveillance program for favorable-risk prostate cancer. *Journal of Clinical Oncology*, page To appear, 2015.
- [44] Jeffrey J. Tosoian, Bruce J. Trock, Patricia Landis, Zhaoyong Feng, Jonathan I. Epstein, and Alan W. Partin. Active Surveillance Program for Prostate Cancer: An Update of the Johns Hopkins Experience. *Journal of Clinical Oncology*, 29:2185–2190, 2011.
- [45] Matthew Truong, Jon A Slezak, Chee Paul Lin, Viacheslav Iremashvili, Martins Sado, Aria A Razmaria, Glen Levenson, Mark S Soloway, Scott E Eggener, E Jason Abel, et al. Development and multi-institutional validation of an upgrading risk tool for gleason 6 prostate cancer. *Cancer*, 119(22):3992–4002, 2013.
- [46] Nicholas J. van As, Andrew R. Norman, Karen Thomas, Vincent S. Khoo, Alan Thompson, Robert A. Huddart, Alan Horwich, David P. Dearnaley, and Christo-

- pher C. Parker. Predicting the probability of deferred radical treatment for localised prostate cancer managed by active surveillance. *European Urology*, 54:1297–1305, 2008.
- [47] Roderick C. N. van den Bergh, Stijn Roemeling, Monique J. Roobol, Gunner Aus, Jonas Hugosson, Antti S. Rannikko, Teuvo L. Tammela, Chris H. Bangma, and Schröder. Outcomes of men with screen-detected prostate cancer eligible for active surveillance who were managed expectantly. *European Urology*, 55:1–8, 2009.
- [48] Zhenke Wu, Maria Deloria-Knoll, Laura L Hammitt, and Scott L Zeger. Partially latent class models for case–control studies of childhood pneumonia etiology. *Journal of the Royal Statistical Society: Series C (Applied Statistics)*, 2015.